Angle-resolved photoemission study of the mixed valence oxide V_6O_{13}: Quasi-one-dimensional electronic structure and its change across the metal-insulator transition

R. Eguchi, T. Yokoya, T. Kiss, Y. Ueda, and S. Shin
Institute for Solid State Physics, University of Tokyo, 5-1-5 Kashiwanoha, Kashiwa, Chiba 277-8581, Japan
(Received 17 December 2001; published 20 May 2002)

We have performed angle-resolved photoemission spectroscopy of mixed valence oxide V_6O_{13} that shows a metal-insulator transition (MIT) at $\simeq 150$ K. In the metallic phase, we observe two bands near the Fermi level (E_F). One is a prominent band located around 0.8 eV and the other is a weak structure around 0.2 eV that shows dispersion toward E_F only along the *b* axis. Furthermore, though the momentum distribution curve at E_F shows a peak at $kb/\pi = 0.29 \pm 0.01$ indicative of a E_F crossing, the intensity of the band near E_F is strongly suppressed in the region of E_F. These observations indicate quasi-one-dimensional electronic states of V_6O_{13}, consistent with a highly anisotropic behavior observed from resistivity and optical conductivity measurements. Across the MIT, the band near E_F shifts to higher binding energy and becomes less dispersive, resulting in opening of an energy gap of 0.2 eV. We discuss some implications of the experimental results.

DOI: 10.1103/PhysRevB.65.205124 PACS number(s): 79.60.−i, 71.10.Pm, 71.30.+h

Most of vanadium oxides exhibit a metal-insulator transition (MIT) as a function of temperature and have been extensively studied in order to understand the mechanism. While, for monovalence vanadium oxides such as VO_2, the mechanism has been discussed in terms of the on-site correlation effect,[1] that of mixed valence oxides has been thought to originate in different mechanism, since electrons in mixed valence oxides can transfer to another site without the effect of the Coulomb energy.[2]

V_6O_{13}, which is classified into the Wadsley phase expressed by V_nO_{2n+1}, is a mixed valence compound and also exhibits a sharp (resistivity changes an order more than 10^4 along all crystal axes) MIT at $T_t \simeq 150$ K (Ref. 3) with an antiferromagnetic order below $T_N \simeq 50$ K.[2,4] V-O bond length analysis of the metallic phase has reported the existence of three different vanadium sites, V(1), V(2), and V(3), with the effective charges of 4.16, 4.60, and 4.34, respectively, indicating of the mixed valences of two V^{4+}- like and one V^{5+}-like sites. Below T_t, it has suggested that the charge redistribution occurs, where V(1) ions become more V^{5+}-like while the V(2) and V(3) ions more V^{4+}-like. Nuclear magnetic resonance (NMR) measurements[2,4] have revealed that, below T_t, half of the V^{4+} sites takes singlet spin pairs resulting in the decrease of the magnetic susceptibility.

The crystal structure of V_6O_{13} is defined as a monoclinic system and changes space group symmetry from $C2/m$ in the metallic phase to $C2$ in the insulating phase (Fig. 1).[5] The crystal consists of distorted VO_6 octahedra, which form two types of sheets parallel to the *a*-*b* plane (*A* and *B* in Fig. 1) including zigzag vanadium chains running along the *b* axis with different arrangement of three vanadium sites V(1), V(2), and V(3) [Figs. 1(b) and 1(c)]. The zigzag vanadium chains of the *A* plane are similar to those of α'-NaV_2O_5 that shows a typical one-dimensional electronic structure.[6] Actually, electrical resistivity of V_6O_{13} measured along the *a*, *b*, and *c* axes of the monoclinic structure shows anisotropic behavior with the lowest resistivity along the *b* axis.[3] This suggests a possibility of one-dimensional-like electronic structures in V_6O_{13}.

In this paper, we report angle-resolved photoemission spectroscopy (ARPES) of mixed valence oxide V_6O_{13} across the MIT. Due to flat and mirrorlike surfaces obtained by cleaving, we could perform ARPES measurements, which investigate momentum-(k) dependent electronic structures. In the metallic phase, we observed two features near the Fermi level (E_F). One is a prominent band located around 0.8-eV binding energy and the other is a weak feature around

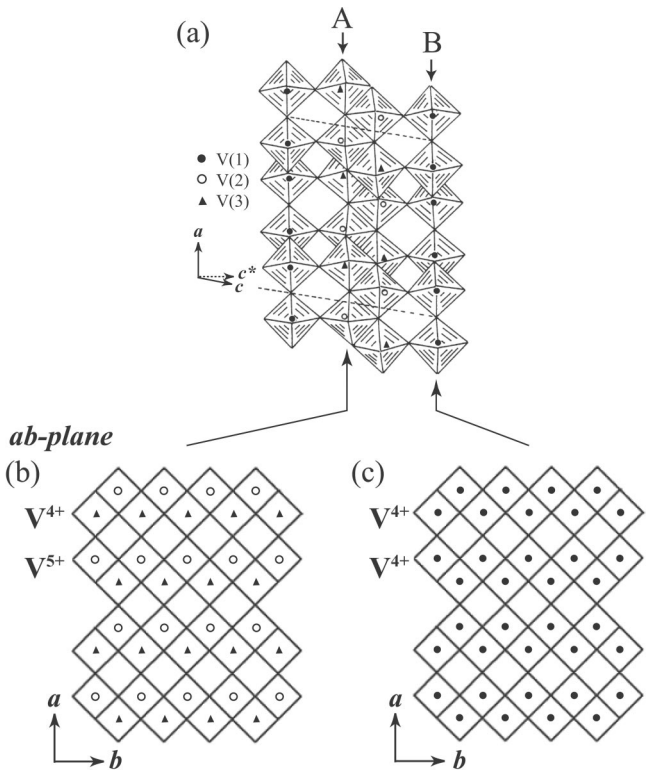

FIG. 1. (a) The crystal structure of V_6O_{13} for the metallic phase, projected on the (010) plane.[5] (b) and (c), two types of *a*-*b* planes, *A* and *B*, including zigzag chains running along the *b* axis with mixed V^{4+}-like and V^{5+}-like sites, and with mono-V^{4+}-like sites, respectively.

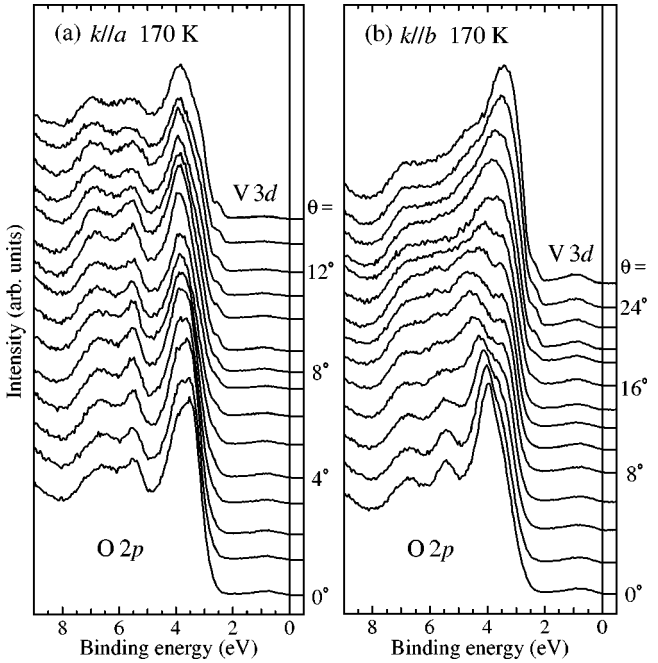

FIG. 2. Valence-band ARPES spectra of V_6O_{13} along (a) the *a* axis and (b) the *b* axis at 170 K.

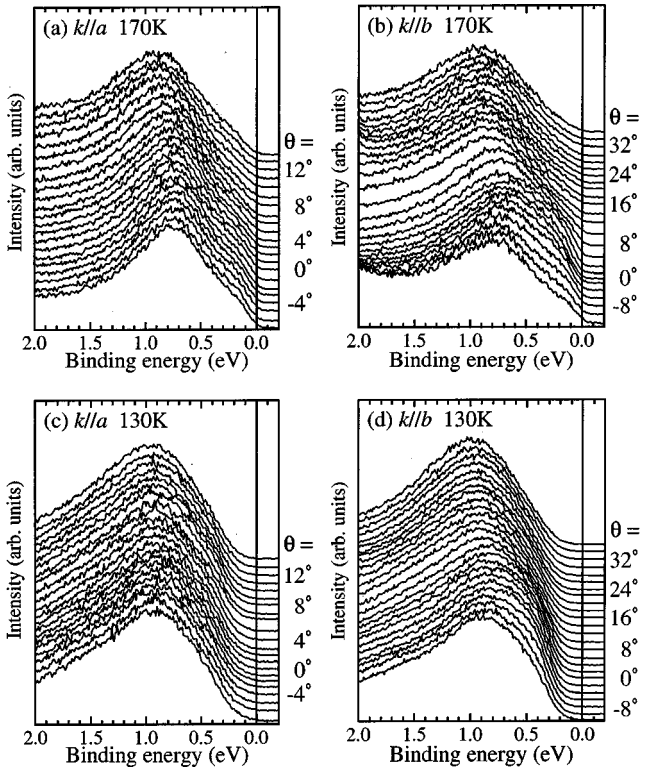

FIG. 3. ARPES spectra of V $3d$ bands of V_6O_{13} along (a) the *a* axis and (b) the *b* axis at 170 K, and along (c) the *a* axis and (d) the *b* axis at 130 K.

0.2 eV showing finite dispersion only along the direction of the zigzag chain. These results are consistent with the resistivity and optical measurements showing highly anisotropic behavior.[3,7] We also observed that the dispersive band looses its intensity near the E_F region, though it has peaks in the momentum distribution curves (MDC's) that relate to the existence of the Fermi momentum (k_F), reminiscent of those of other typical one-dimensional systems. Across the MIT, both the bands shift to higher binding energy with the band near E_F having a larger shift, resulting in opening of a gap having $\sim$0.2 eV. These results represent the electronic structure and its change across the MIT of the mixed valence oxide V_6O_{13}.

V_6O_{13} single crystals were grown by chemical transport reaction using $TeCl_4$ as a transport agent.[3] Details are as follows: About 10 g of V_6O_{13} powder prepared using ceramic method and 500 mg of $TeCl_4$ were sealed in an evacuated transparent silica tube with the dimension of 150 mm in length and 30 mm in diameter. This tube was held in a horizontal furnace with the growth zone at 550 °C and the charge zone at 600 °C for a week.

ARPES experiments were carried out on a photoemission spectrometer having a Scienta SES2002 analyzer, a He discharging lamp (GAMMADATA) with a monochromator, and a flowing liquid-He cryostat with a thermally shielded sample holder. The energy and angular resolutions for the He Iα resonance line were set to 15 meV and $\pm 0.1°$, respectively, to get reasonable count. V_6O_{13} samples were cleaved *in situ* parallel to the (001) plane and all spectra were recorded within 30 min after cleaving. The measurements were done at 170 K for the metallic phase and 130 K for the insulating phase. We could not measure below T_N because of charging effects. E_F of V_6O_{13} was referenced to that of a gold film evaporated onto the sample holder.

Figure 2 shows two sets of valence-band ARPE spectra of V_6O_{13} measured along (a) the *a* axis and (b) the *b* axis at 170 K, latter of which corresponds to the direction of the zigzag chain. Normalization of the spectral intensity is made at an binding energy of 8 eV. The angles indicated at the right side of selected spectra are the polar angle relative to the surface normal. These spectra are very similar to the angle-integrated spectra of V_6O_{13}.[8] The valence-band spectrum at 0° has prominent features from 3 eV to 8 eV with mainly three structures and has a very weak feature around 1 eV. The former features are ascribed to O $2p$ dominant bands, while the latter is ascribed to V $3d$ dominant bands. The O $2p$ bands measured along the a axis [Fig. 2(a)] have a negligible dispersion within the first Brillouin zone ($\theta \simeq 7°$ corresponds to the zone boundary). In sharp contrast, those along the *b* axis [Fig. 2(b)] change in relative intensity and peak position as θ is increased, indicating large k dependence in the electronic structure. The sharp structure at 4 eV that has minimum binding energy at 0° moves to higher binding energy till around $\theta \simeq 12°$, but it moves back for higher θ. The periodicity of the valence-band dispersion match the size of the Brillouin zone along the *b* axis, indicating that the present spectra reflect bulk electronic states of V_6O_{13}. Having a two-dimensional network in the *a*-*b* plane, the O $2p$ states hybridizing with the V $3d$ states reflect the electronic structures of the V $3d$ sites arranged in the one-dimensional manner. This result indicates that the electronic structure of V_6O_{13} is highly anisotropic within the *a*-*b* plane.

In Fig. 3, we show ARPE spectra near E_F measured along

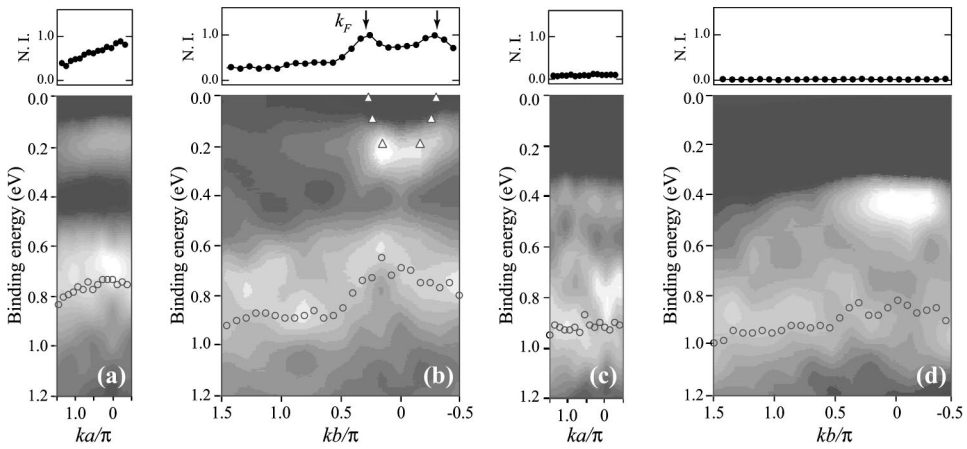

FIG. 4. Second derivative intensity maps near E_F of V_6O_{13} obtained from ARPES spectra measured along (a) the *a* axis and (b) the *b* axis at 170 K, and along (c) the *a* axis and (d) the *b* axis at 130 K. Lighter areas correspond to bands. Triangles in (b) indicate peak positions from MDC's at 0.0, 0.1, and 0.2 eV. Circles indicate the peak positions of the prominent structure from Fig. 3. Upper panels show MDC's at E_F.

the *a* axis and *b* axis at 170 K [(a) and (b)] and at 130 K [(c) and (d)] across T_t. The intensity of each spectrum is normalized with the integrated intensity from -0.1 eV to 1.8 eV. First, we concentrate on the spectral behavior of the metallic phase [Figs. 3(a) and 3(b)]. For both directions, we observed prominent features around 0.8 eV, which looks similar to the lower Hubbard band, as has been observed in other vanadium oxides.[9] We also observe a weak shoulder feature around 0.2 eV especially along the *b* axis. Along the *a* axis, the band at 0.8 eV has almost no dispersion within the Brillouin zone, while, along the *b* axis, the bands are found to have dispersion. For example, energy position of the prominent peak gradually moves towards higher binding energy as θ is increased from 0° to 12°. The observed difference in band dispersion near E_F is consistent with the anisotropic behavior as seen in the valence-band region (Fig. 2) and most likely originates in the zigzag chains running along the *b* axis (Fig. 1). Furthermore, as seen in Figs. 3(a) and 3(b), the intensity near E_F is strongly reduced and the spectra do not have a Fermi edge, though those spectra were measured in the metallic phase. We will discuss this latter.

In order to look at the band structure near E_F, we took the second derivative of raw data shown in Fig. 3 after moderate smoothing and plotted the intensity as a function of the momentum and the binding energy (Fig. 4). Since this analysis makes the curvature of the law ARPES spectra having some important information clearer, it has been taken for other ARPES results.[10–12] Lighter areas correspond to bands. We observe two bands, which is directly related to the two structures in the raw spectra shown in Fig. 3 (the prominent band at 0.8 eV and the weak features at about 0.2 eV). As is clearly seen from Fig. 4, the dispersion of the band near E_F is different between the *a* and *b* axis. The band near E_F along that the *a* axis is almost flat having a maximum energy position around $ka/\pi=0$ and shows no E_F crossings within the Brillouin zone. In contrast, that along the *b* axis seems to have upward dispersion tending toward E_F. However, the second derivative intensity near E_F disappears, which relates to the absence of Fermi edge structures in the raw spectra, though the system is in the metallic phase. One might speculate that the surface of this materials is not metallic, as has been reported for other vanadium oxides.[13] To confirm the band dispersion near E_F, we have done MDC analysis of the raw data shown in Fig. 3. The MDC at E_F along the *b* axis [Fig. 4(b), upper panel] shows two peaks to be symmetrical with respect to $kb/\pi=0$. Further we have found that the peak positions of MDC for other binding energies, which relates to the band dispersion, form a small electron pocket at $kb/\pi=0$, as shown with triangles in Fig. 4(b). Observed spectral behavior is reminiscent to that of quasi-one-dimensional materials. For example, it is reported that ARPES results of quasi-one-dimensional charge-density wave material $K_{0.3}MoO_3$ exhibit the E_F weights suppression though there are E_F crossings,[14] and such a spectral shape has been discussed in terms of Tomonaga-Luttinger liquid. Furthermore, present ARPES results of V_6O_{13} are consistent with highly anisotropic behavior observed from resistivity[3] and recent optical conductivity measurements.[7] Thus the absence of the Fermi edge is most likely reflecting the bulk electronic states, indicating the quasi-one-dimensional-like electronic structure along the *b* axis.

From the value of k_F, we could speculate the relation between the observed two electronic structures and two types of the zigzag chains. As shown in Fig. 4(b), k_F along the *b* axis is located around $kb/\pi=0.29\pm0.01$. The zigzag chains with mono-V^{4+} sites in the *A* planes and mixed V^{4+} and V^{5+} sites in the *B* planes (see, Fig. 1) can be considered as the nearly half-filled and quarter-filled two-leg ladder cases, respectively. Normally, the two-leg ladder has two bands attributed to bonding and antibonding bands from two rows, whose energy separation is determined by the hopping integral between the two rows. For the monozigzag chains, one might observe a peak in a MDC located around $kb/\pi=0.42$ for smaller separation of the two bands, but two peaks that are symmetrical with respect to $kb/\pi=0.42$ for larger separation. On the other hand, for the mixed zigzag chains, one might observe a peak in a MDC located around $kb/\pi=0.26$ for smaller separation of the two bands, but two peaks that are symmetrical with respect to $kb/\pi=0.26$ for larger separation. The observed value of $kb/\pi=0.29\pm0.01$ is close to that expected for mixed zigzag chains. Thus it is more plausible to say that the band near E_F is derived from the zigzag chains with mixed V^{4+} and V^{5+} sites. The fact that we do not distinguish the bonding and antibonding bands from the present study indicates that the energy separation

between the two bands, which corresponds to the hopping integral between the two chains, are not so large.

Lastly, we discuss the spectral change across the MIT. Figures 3(c) and 3(d) show the spectra in the insulating phase along the *a* and *b* axis measured at 130 K, respectively. From comparison with the band dispersions measured at the metallic phase, we can observe change in electronic structures. The intensity of the band near E_F observed in the metallic phase becomes smaller in the insulating phase, resulting in opening of a gap of nearly 0.2 eV along the both directions. The shift of this band through the MIT is very similar to the previous result observed in angle-integrated photoemission.[8] The 0.8-eV band in the insulating phase becomes broader and seems to have less dispersion compared to that in the metallic phase. These spectral behaviors are more evident in the second derivative plots as shown in Figs. 4(c) and 4(d), where the band near E_F in the metallic phase seems to shift to ~ 0.4 eV in the insulating phase. The opening of the gap is further confirmed from the MDC's at E_F showing that intensity at E_F in the insulating phase is strongly reduced compared to that in the metallic phase. These observations in energy distribution curves and MDC's clearly indicate the change in the electronic structures across the MIT, consistent with the bulk metal-insulator transition. In addition, we observe that the dispersion of the 0.8-eV bands becomes smaller in the insulating phase than in the metallic phase, as is seen from the open circles in the Fig. 4.

NMR and x-ray diffraction measurements have revealed important changes across the MIT. From x-ray diffraction measurements,[5] it has reported that the lattice parameters of the *a* and *b* axis increase while that of *c* axis decrease below T_t, namely, the V-V separations in the *a-b* plane increase while those along the *c* axis decrease. Further, a V-O bond length analysis has reported that the V(1) ions become more V^{5+}-like while the V(2) and V(3) ions become more V^{4+}-like in the insulating phase, indicating the occurrence of rearrangement of charge distribution through T_t.[5] NMR study has showed that half of the V^{4+} sites takes singlet spin pairs giving rise to the decrease of the magnetic susceptibility.[2,4] For V_4O_7, which is another mixed valence vanadium oxide exhibiting a MIT, pairing of V sites rather than the on-site electron correlation plays an important role in the MIT.[15] Even for V_6O_{13}, the on-site correlation may not be a proper candidate, since the band at E_F of V_6O_{13} is not a half-filled case that is a necessary condition for the Mott transition. Neither may it be possible to attribute the opening of the gap of 0.2 eV from the present measurements to the spin pairing reported from the NMR study alone, because the energy gain due to a spin pairing is a order of several tenth meV. Rather the observed drastic change of the bands with flatter dispersions in the insulating phase seems reflecting the redistribution through T_t and the simultaneous change in lattice parameters, both of which with cooperative manner may lead to the enhancement of the charge localization in the vanadium sites that give rise to the MIT.

In conclusion, we have investigated the electronic structures of mixed valence vanadium oxide V_6O_{13} using ARPES. ARPES data show the dispersive band near E_F only along the *b* axis, which is the direction of zigzag chains, with suppressed intensity near E_F. This agrees with the highly anisotropic behavior observed from resistivity and optical conductivity measurements and thus indicates that the electronic structure of V_6O_{13} is quasi-one-dimensional-like. Across the MIT, we observed the energy shifts of the two bands near E_F with change in dispersion, which result in opening of the energy gap of 0.2 eV. These results show the momentum resolved electronic structures of mixed valence vanadium oxide V_6O_{13}. We hope that the present results motivate further theoretical studies to understand the mechanism of the MIT in V_6O_{13}.

We thank Dr. A. Chainani for stimulating discussion. We also thank professor T. Tohyama for valuable comments. This work was supported by Grant-in-Aid for Scientific Research from the Ministry of Education, Culture, Sports, Science and Technology of Japan. T.K. thanks the JSPS for financial support.

[1] A. Zylbersztejin and N.F. Mott, Phys. Rev. Lett. **11**, 4383 (1975).
[2] A.C. Gossard, F.J.D. Salvo, L.C. Erich, J.P. Remeika, H. Yasuoka, K. Kosuge, and S. Kachi, Phys. Rev. B **10**, 4178 (1974).
[3] K. Kawashima, Y. Ueda, K. Kosuge, and S. Kachi, J. Cryst. Growth **26**, 321 (1974).
[4] M. Ito, H. Yasuoka, Y. Ueda, and K. Kosige, J. Phys. Soc. Jpn. **53**, 1847 (1984).
[5] P.D. Dernier, Mater. Res. Bull. **9**, 955 (1974).
[6] K. Kobayashi, T. Mizokawa, A. Fujimori, M. Isobe, and Y. Ueda, Phys. Rev. Lett. **80**, 3121 (1998).
[7] R. Eguchi, T. Yokoya, T. Kiss, Y. Ueda, H. Tajima, J. Yamazaki, and S. Shin, Physica B **312-313**, 600 (2002).
[8] S. Shin, S. Suga, M. Taniguchi, M. Fujisawa, H. Kanzaki, A. Fujimori, H. Daimon, Y. Ueda, K. Kosuge, and S. Kachi, Phys. Rev. B **41**, 4993 (1990).
[9] A. Fujimori, I. Hase, H. Namatame, Y. Fujishima, Y. Tokura, H. Eisaki, S. Uchida, K. Takegahara, and F.M.F. de Groot, Phys. Rev. Lett. **69**, 1796 (1992).
[10] T. Takahashi, T. Yokoya, A. Ashihara, O. Akaki, H. Fujisawa, A. Chainani, M. Uehara, T. Nagata, J. Akimitsu, and H. Tsunetsugu, Phys. Rev. B **56**, 7870 (1997).
[11] A.V. Puchkov, Z.-X. Shen, T. Kimura, and Y. Tokura, Phys. Rev. B **58**, R13 322 (1998).
[12] R. Claessen, M. Sing, U. Schwingenschlogl, P. Blaha, M. Dressel, and C.S. Jacobsen, Phys. Rev. Lett. **88**, 096402 (2002).
[13] K. Maiti, P. Mahadevan, and D.D. Sarma, Phys. Rev. Lett. **80**, 2885 (1998).
[14] G.-H. Gweon, J.W. Allen, R. Claessen, J.A. Clack, D.M. Poirier, P.J. Benning, C.G. Olson, W.P. Ellis, Y.-X. Zhang, L.F. Schneemeyer, J. Marcus, and C. Schlenker, J. Phys.: Condens. Matter **8**, 9923 (1996).
[15] A.C. Gossard, J.P. Remeika, T.M. Rice, H. Yasuoka, K. Kosuge, and S. Kachi, Phys. Rev. B **9**, 1230 (1974).